3-8-2010

MicroRNA-31 Functions as an Oncogenic MicroRNA in Mouse and Human Lung Cancer Cells by Repressing Specific Tumor Suppressors

Xi Liu
Dartmouth College

Lorenzo F. Sempere
Dartmouth College

Haoxu Ouyang
Dartmouth College

Vincent A. Memoli
Dartmouth College

Angeline S. Andrew
Dartmouth College

MicroRNA-31 functions as an oncogenic microRNA in mouse and human lung cancer cells by repressing specific tumor suppressors

Xi Liu,[1,2] Lorenzo F. Sempere,[2,3] Haoxu Ouyang,[1,2] Vincent A. Memoli,[2,4,5] Angeline S. Andrew,[2,5,6] Yue Luo,[1,2] Eugene Demidenko,[2,5,6] Murray Korc,[1,2,3,5] Wei Shi,[1,2] Meir Preis,[2,3] Konstantin H. Dragnev,[2,3,5] Hua Li,[1,2] James DiRenzo,[1,2,5] Mads Bak,[7] Sarah J. Freemantle,[1,2] Sakari Kauppinen,[8,9] and Ethan Dmitrovsky[1,2,3,5]

[1]Department of Pharmacology and Toxicology, Dartmouth Medical School, Hanover, New Hampshire. [2]Dartmouth-Hitchcock Medical Center, Lebanon, New Hampshire. [3]Department of Medicine, [4]Department of Pathology, [5]Norris Cotton Cancer Center, and [6]Department of Community and Family Medicine, Dartmouth Medical School. [7]University of Copenhagen, Denmark. [8]Santaris Pharma, Hørsholm, Denmark. [9]Copenhagen Institute of Technology, Aalborg University, Ballerup, Denmark.

MicroRNAs (miRNAs) regulate gene expression. It has been suggested that obtaining miRNA expression profiles can improve classification, diagnostic, and prognostic information in oncology. Here, we sought to comprehensively identify the miRNAs that are overexpressed in lung cancer by conducting miRNA microarray expression profiling on normal lung versus adjacent lung cancers from transgenic mice. We found that miR-136, miR-376a, and miR-31 were each prominently overexpressed in murine lung cancers. Real-time RT-PCR and in situ hybridization (ISH) assays confirmed these miRNA expression profiles in paired normal-malignant lung tissues from mice and humans. Engineered knockdown of miR-31, but not other highlighted miRNAs, substantially repressed lung cancer cell growth and tumorigenicity in a dose-dependent manner. Using a bioinformatics approach, we identified miR-31 target mRNAs and independently confirmed them as direct targets in human and mouse lung cancer cell lines. These targets included the tumor-suppressive genes large tumor suppressor 2 (*LATS2*) and PP2A regulatory subunit B alpha isoform (*PPP2R2A*), and expression of each was augmented by miR-31 knockdown. Their engineered repression antagonized miR-31–mediated growth inhibition. Notably, miR-31 and these target mRNAs were inversely expressed in mouse and human lung cancers, underscoring their biologic relevance. The clinical relevance of miR-31 expression was further independently and comprehensively validated using an array containing normal and malignant human lung tissues. Together, these findings revealed that miR-31 acts as an oncogenic miRNA (oncomir) in lung cancer by targeting specific tumor suppressors for repression.

Introduction

MicroRNAs (miRNAs) are critical regulators of gene expression (1, 2). Mature miRNAs bind target mRNAs at complementary sites in 3′–untranslated regions (3′-UTRs) or coding sequences and thereby trigger downregulation, suppressing target gene expression (3, 4). MiRNAs are differentially expressed in human cancers and play important roles in carcinogenesis (5). Also, miRNA expression profiles improve cancer classification, diagnosis, and clinical prognostic information (6, 7).

Lung cancer is the most common cause of cancer-related mortality for men and women in the United States (8). Some miRNAs are deregulated in lung cancers. For example, low expression of let-7a and high expression of miR-155 are associated with a poor clinical outcome in lung cancer (9, 10). The miR-34 family is also repressed in cancer and involved in p53 tumor suppression in diverse cancers (11–16), including lung cancer, as our team reported (17). These findings underscored the need for an in-depth search for miRNAs overexpressed in lung carcinogenesis that play critical roles in regulating lung cancer growth or tumorigenicity. This was the objective of the present study.

Our prior work revealed a subset of miRNAs repressed in murine lung cancers relative to adjacent normal lung in cyclin E–transgenic lines and in paired human normal-malignant lung tissues (17). These murine transgenic lines recapitulated frequent features of human lung carcinogenesis, including chromosome instability, hedgehog pathway activation, pulmonary dysplasia, and single, multiple, or metastatic lung adenocarcinomas (18). These models proved useful for identifying repressed miRNAs in murine malignant versus normal lung tissues (17). These findings provided a rationale for confirming similar miRNA expression profiles in human lung cancer (17). The present study sought to use these transgenic lines and a paired human normal-malignant lung tissue bank (17) as well as a normal lung-lung cancer tissue microarray to determine miRNAs prominently overexpressed in lung cancers relative to adjacent normal lung tissue. It was hypothesized that some of these miRNAs would function as oncomirs (oncogenic miRNAs) and critical regulators of lung cancer growth or tumorigenicity.

We performed comprehensive miRNA microarray analyses on pulmonary adenocarcinomas versus adjacent normal lung tissues in transgenic cyclin E–expressing transgenic lines (18) using murine and human annotated miRNAs and a previously described miRNA expression array (17). A novel set of overexpressed miRNAs was found that included miR-31, which was one of the most sub-

Conflict of interest: The authors have declared that no conflict of interest exists.
Citation for this article: *J Clin Invest.* 2010;120(4):1298–1309. doi:10.1172/JCI39566.

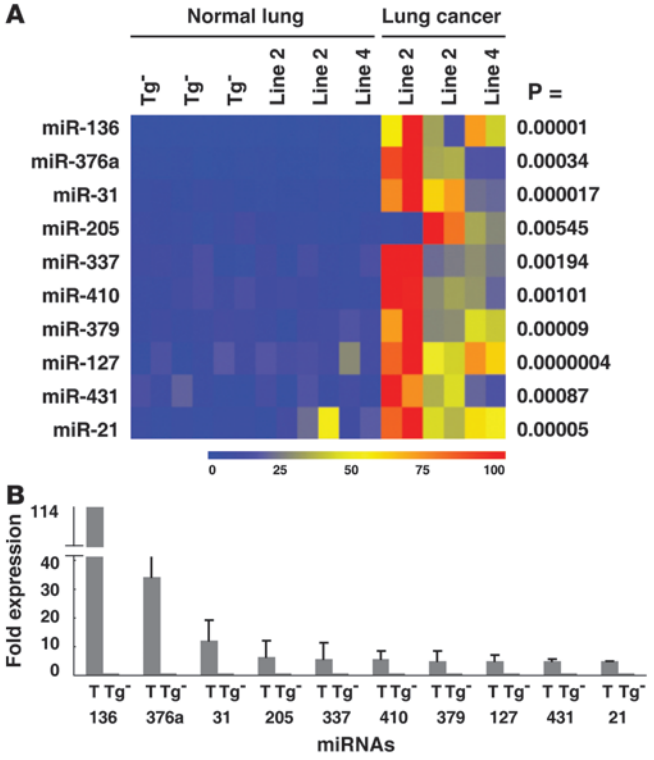

Figure 1
The most prominently overexpressed miRNAs in murine transgenic lung cancers relative to adjacent normal lung tissues. (**A**) MiRNA profiling of lung adenocarcinomas and adjacent normal lung tissues from murine wild-type (line 2) and degradation-resistant (line 4) cyclin E–transgenic lines. As shown, miR-136, miR-376a, miR-31, miR-205, miR-337, miR-410, miR-379, miR-127, miR-431, and miR-21 were each significantly overexpressed in lung adenocarcinomas versus normal lung. (**B**) Quantification of the overexpressed miRNAs in murine lung cancers versus normal lung tissues in **A**. Error bars indicate SD. T, malignant tumor; Tg⁻, murine nontransgenic FVB normal lung tissue.

stantially overexpressed miRNAs in both murine and human lung cancers. Real-time RT-PCR assays and in situ hybridization (ISH) assays were independently performed on specific highlighted miRNAs to confirm findings in both paired murine and human normal-malignant lung tissues. For assessment of the functional consequence of this miRNA overexpression profile, each highlighted miRNA was independently knocked down in murine and human lung cancer cell lines. Only engineered repression of miR-31 conferred growth inhibition of these lung cancer cells.

These findings were extended to the in vivo setting by dose-dependent knockdown of miR-31 in murine lung cancer cells before tail vein injections into syngeneic FVB mice. Large tumor suppressor 2 (*Lats2*) and PP2A regulatory subunit B alpha isoform (*Ppp2r2a*) were also identified bioinformatically as tumor-suppressive miR-31 target mRNAs. Luciferase reporter assays revealed that both LATS2 and PPP2R2A were miR-31 direct targets through 3′-UTR binding. Mechanistic evidence in support of functional roles for LATS2 and PPP2R2A in triggering miR-31 effects was found. Further evidence for the relevance of LATS2 and PPP2R2A expression in lung carcinogenesis came independently from studies of their expression profiles in a panel of murine and human lung cancers relative to adjacent normal lung tissues. These observations were validated in tissue microarray studies of lung cancer cases enrolled in a population-based epidemiologic study from the New Hampshire State Cancer Registry and the Dartmouth-Hitchcock Tumor Registry. Taken together, these findings indicate that miR-31 acts as an oncomir by repressing expression of specific tumor suppressors in lung cancer.

Results

Overexpression of miRNAs in murine transgenic lung cancer. To uncover miRNAs overexpressed in lung cancers, we conducted comprehensive locked nucleic acid (LNA) microarray analyses to obtain miRNA expression profiles independently in malignant and normal lung. Tissues were isolated from human surfactant protein C–driven (SP-C–driven) wild-type and proteasome degradation–resistant cyclin E–transgenic murine lines (18). Degradation-resistant cyclin E lines had a higher number of neoplastic lesions as compared with wild-type cyclin E lines even when cyclin E expression levels were comparable (18). Adenocarcinomas and adjacent normal lung tissues from these transgenic lines and normal lung tissues from age- and sex-matched nontransgenic (Tg^-) FVB mice were each examined in these miRNA microarrays containing 315 murine miRNAs. Three transgenic mice and 3 Tg^- mice were independently examined in miRNA microarray analyses. Figure 1A displays statistically significant expression changes of the most- to least-overexpressed miRNAs in these representative murine tissues. Figure 1B presents the fold changes of these miRNAs relative to Tg^- normal lung tissues.

These lung cancers had 114- to 4-fold higher expression levels of the highlighted miRNAs as compared with Tg^- normal lung tissues. The 3 miRNAs with highest expression levels (>10 fold) in these lung cancers were miR-136, miR-376a, and miR-31, as shown in Figure 1B. All 3 miRNAs were previously unrecognized as highlighted miRNAs in lung cancer. Several of the overexpressed miRNAs identified in this study were concordant with previously reported miRNA profiles in malignant versus normal tissues (19–26). Of note, miR-21 expression was reported as being increased in lung cancer (27). As expected, miR-21 expression in transgenic lung cancers was much higher (5-fold) in these tumors relative to adjacent normal lung, as shown in Figure 1.

To independently validate and to determine spatial distribution patterns of specific miRNAs, we used ISH assays. As shown in Figure 2, malignant (adenocarcinoma) and adjacent normal lung tissues were studied in cyclin E–transgenic mice. Histopathologic analyses of lung tissues were performed to confirm that normal and malignant lung tissues were each examined. Expression profiles of miR-31 (the functionally highlighted miRNA), miR-21, and control 18S rRNA were each analyzed by ISH in malignant and normal lung tissues from transgenic mice. As shown, miR-31 exhibited reduced expression in murine normal lung tissue, but high miR-31 expression was detected within murine malignant lung tissue. Concordant results were observed in human paired normal-malignant lung tissues, as shown in Figure 2. Low levels of miR-31 expression were found in normal human lung tissue, but a high expression level was present in malignant lung tissue. As anticipated from previous work (17, 27), miR-21 was also detected at higher expression levels in malignant than in normal human lung tissue (Figure 2). The 18S rRNA signal was ubiquitously expressed in both normal and malignant lung tissues, confirming

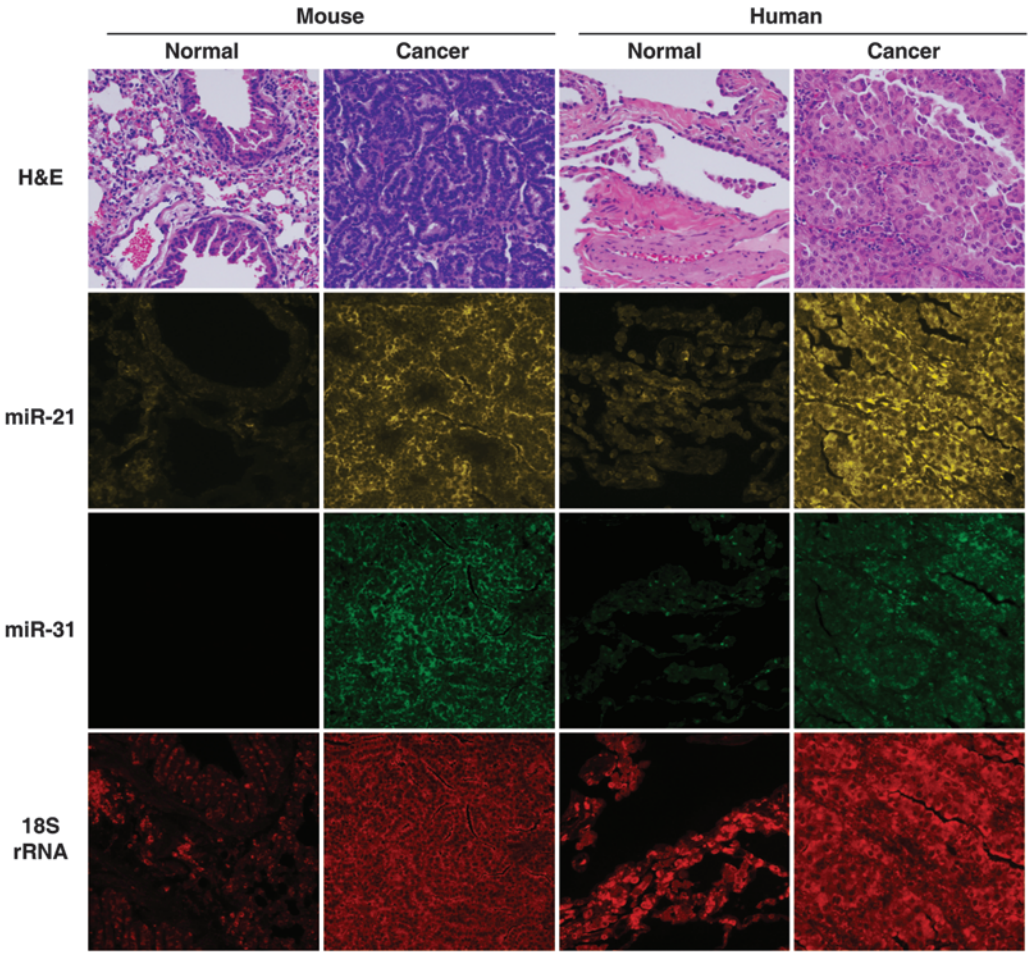

Figure 2
ISH assays for representative overexpressed miRNAs in lung cancers. These assays were conducted on adenocarcinomas and adjacent normal lung tissues from cyclin E–transgenic mice and from human paired normal-malignant lung tissues. Overexpression of miR-21 and miR-31 was detected in malignant versus normal lung tissues. The 18S rRNA signal served as a positive control for integrity of RNA. H&E staining of the indicated tissue sections is shown. Original magnification, ×100.

integrity of the RNA used in these tissue analyses. Together, these results confirmed differential expression of specific miRNAs in malignant versus normal lung tissues.

To validate the expression profiles of these miRNAs independently, we conducted real-time RT-PCR assays using total RNA isolated from pulmonary adenocarcinomas and adjacent normal lung tissues from the described murine transgenic lines. As shown, miR-136, miR-376a, miR-31 (Figure 3), and other miRNAs (data not shown) were each significantly overexpressed relative to Tg^- normal lung tissues by real-time RT-PCR assays using RNA derived from transgenic malignant versus normal transgenic or Tg^- lung tissues. Each assay was conducted at least 3 independent times, with similar results obtained. Results were consistent with findings from miRNA microarray experiments (Figure 3A and data not shown). The findings shown in Figure 3A from murine lung tissues are presented, since the same miRNAs were also frequently overexpressed in human lung cancers versus adjacent normal lung tissues, as shown in Figure 3B.

Overexpression of miRNAs in human lung cancers. Since previous work demonstrated that expression profiles for murine tumor-suppressive miRNAs were concordant with those detected in human lung cancers (17), it was hypothesized that augmented miRNAs identified in murine lung cancers would also be overexpressed in human lung cancers as compared with adjacent normal lung tissues. To explore this possibility, we examined paired human normal-malignant lung tissues from subsets of non–small cell lung cancers (NSCLCs: adenocarcinoma, squamous cell carcinoma, large cell carcinoma, and bronchoalveolar carcinoma) using a previously described lung tissue bank (17, 28). Overexpression of miR-136, miR-376a, and miR-31 was frequently detected in each type of NSCLC as compared with adjacent normal lung tissues (Figure 3B). Each of these highlighted miRNAs was independently examined in the indicated murine and human lung tissues. In contrast, the other miRNAs identified as differentially overexpressed in murine transgenic lung cancer (Figure 1) were detected as overexpressed in only a minority of these NSCLC subtypes (data not shown). Of these differentially overexpressed miRNAs, miR-31 was selected for in-depth study based on the transfection experiments described below.

Knockdown of miRNAs in lung cancer cells. To study whether these highlighted miRNAs affected lung cancer growth, we conducted independent experiments to engineer the miRNAs with increased

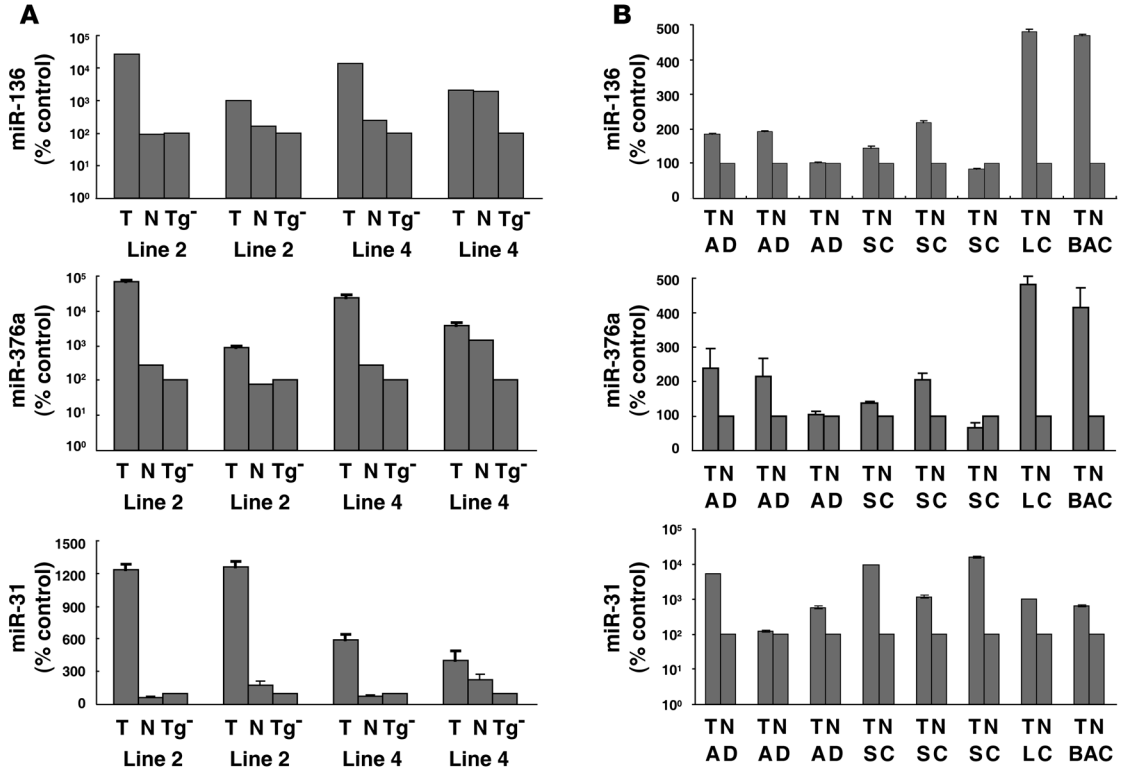

Figure 3

Validation of miR-136, miR-376a, and miR-31 expression profiles by real-time RT-PCR assays performed on RNA isolated from the indicated murine cyclin E–transgenic lines and from paired human normal-malignant lung tissues. (**A**) Real-time RT-PCR assays for miR-136, miR-376a, and miR-31 were performed. T, malignant tumor; N, adjacent normal murine lung; and Tg⁻, murine nontransgenic FVB normal lung tissue. Results were normalized to expression levels detected in FVB murine Tg⁻ lung tissues. (**B**) Real-time RT-PCR assays for miR-136, miR-376a, and miR-31 were independently performed on paired human normal-malignant lung tissues. AD, adenocarcinoma; SC, squamous cell carcinoma; LC, large cell carcinoma; BAC, bronchoalveolar carcinoma. Results were normalized to expression levels measured in normal human lung. Error bars indicate SD.

or decreased expression in murine lung cancer cell lines (ED-1 and ED-2) as well as in the murine C10 alveolar type II epithelial cell line. Independent overexpression of miR-136, miR-376a, and miR-31 in these cell lines did not appreciably affect murine lung cell growth (data not shown). This was likely due to the high basal levels of these miRNAs in these respective cell lines: engineering them to express even higher levels did not elicit further effects. To confirm this, we independently conducted real-time RT-PCR assays in each of these cell lines as well as in murine and human lung cancer tissues to assess the relative levels of the miRNAs of interest as compared with control RNAs (small nucleolar RNA-135 [sno-135] for murine cells and tissues and U6 small nuclear 2 RNA [RUN6B] for human cells and tissues). Findings revealed that miR-31 expression levels were higher in nearly all the cell lines examined (cancer and immortalized cell lines) than in the murine (Supplemental Figure 1A; supplemental material available online with this article; doi:10.1172/JCI39566DS1) or human (Supplemental Figure 1B) lung cancer tissues.

In contrast, knockdown of miR-31 significantly reduced lung cancer cell growth as compared with controls, as shown in Figure 4A. Independent knockdown of miR-31 was achieved in murine lung cancer cell lines (ED-1 and ED-2) as well as in murine C10 pulmonary epithelial cells. ED-1 and ED-2 cell growth was suppressed more than 60% ($P < 0.0001$), while C10 cell growth was less prominently reduced ($P < 0.01$). An appreciable increase in apoptosis was not observed by knockdown of miR-31 as compared with controls (data not shown). Greater than 90% of cells from each cell line were transfected (data not shown), and miR-31 levels in each knockdown transfectant were reduced to less than 10% of the control transfectants, as confirmed by real-time RT-PCR assays (Figure 4A).

It was hypothesized that similar effects would be observed in BEAS-2B human immortalized bronchial epithelial cells versus human lung cancer cell lines. The same transfection experiments were independently conducted in H23 and H226 human lung cancer cell lines as well as in BEAS-2B immortalized human bronchial epithelial cells. A significant ($P = 0.00019$ for H23 cells and $P = 0.015$ for H226 cells) growth-suppressive effect was independently caused by knockdown of miR-31 in H23 and H226 cells (Figure 4A). Intriguingly, proliferation of transfected BEAS-2B cells was not significantly affected by engineered miR-31 knockdown, suggesting a different response to loss of miR-31 expression in human immortalized versus malignant lung cells. Cell cycle analyses were conducted on transfectants. G_1 arrest was observed in murine and human lung cancer cell lines (data not shown).

To exclude nonspecific transfection effects and to examine whether this growth inhibition was reversible, miR-31 was independently knocked down in ED-1 and ED-2 cells and growth sup-

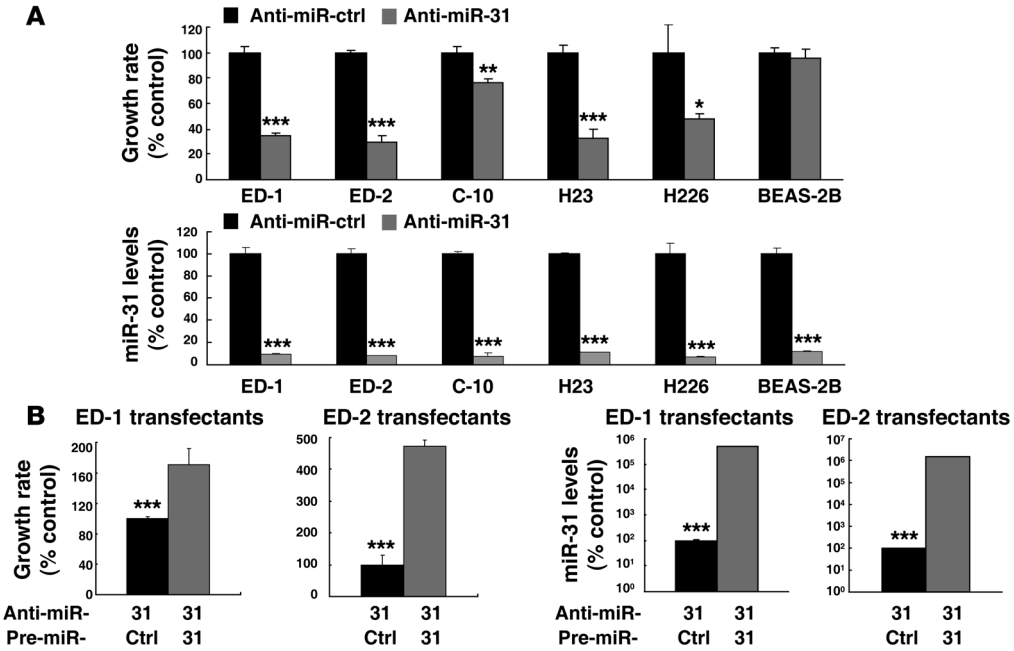

Figure 4

Regulation of miR-31 expression affects lung cancer cell proliferation. (**A**) Proliferation of ED-1 and ED-2 murine lung cancer cells and H23 and H226 human lung cancer cells was suppressed by engineered miR-31 knockdown after anti–miR-31 transfection, but murine C10 pulmonary epithelial cell proliferation was suppressed to a lesser extent. BEAS-2B human immortalized bronchial epithelial cell growth was not significantly reduced by this transfection. $^{*}P < 0.05$, $^{**}P < 0.01$, $^{***}P < 0.0001$. The lower panel displays results of real-time RT-PCR assays that confirm miR-31 repression; $^{***}P < 0.0001$. (**B**) Significant repression of ED-1 and ED-2 cell growth caused by anti–miR-31 was antagonized by transfection of pre–miR-31 at 48 hours after anti–miR-31 transfection. The left panels display proliferation, and the right panels present the real-time RT-PCR assay results confirming the expected repressed levels of these miR-31 transfectants as compared with control transfectants (Ctrl). $^{***}P < 0.0001$. Error bars indicate SD.

pression examined in these transfectants. Two days after the first transfection, pre–miR-31 or an inactive pre-miR control oligonucleotide was transiently overexpressed in these cells. As expected, engineered overexpression of miR-31 reversed anti–miR-31–mediated growth suppression (Figure 4B). The miR-31 expression levels in the indicated transfectants were determined by real-time RT-PCR assays (Figure 4B).

Knockdown of miR-31 represses in vivo tumorigenicity. It was examined whether miR-31 inhibition would reduce clonal growth of lung cancer cells. This was based on the observation that miR-31 knockdown inhibited lung cancer cellular growth. Consistent with the hypothesis, independent knockdown of miR-31 was found to significantly reduce ED-1 and ED-2 colony formation, as shown in Figure 5A. Anti–miR-31 transfectants had significantly fewer colonies than the controls, with $P = 0.018$ for ED-1 cells and $P = 0.0002$ for ED-2 cells.

To examine whether the observed repression of lung cancer cell clonal growth was associated with repression of in vivo tumorigenicity, we injected syngeneic FVB mice via tail vein with ED-1 cells (see Methods) that were transiently transfected with anti–miR-31 to achieve knockdown of miR-31. Results were compared with those for control transfectants. Twenty-five days after tail vein injections, lung lesions were scored. As shown in Figure 5B, ED-1 cells transfected with anti–miR-31 produced significantly fewer ($P \leq 0.05$) lung lesions as compared with ED-1 control transfectants. Knockdown of miR-31 by transient transfection persisted for 5–6 days, while the outgrowth of lung lesions occurred typically by 7–15 days after injection (data not shown). To examine whether higher anti–miR-31 transfection dosages produced greater repression of miRNA-31 expression or in vivo tumorigenicity, we transfected ED-1 cells with 4-fold-higher dosages of anti–miR-31 or anti–miR control oligonucleotides than those used in Figure 5B. Compared with controls and with the results of the anti–miR-31 ED-1 transfection experiment shown in Figure 5B, findings revealed that a higher anti–miR-31 transfection dosage reduced miR-31 expression and in vivo lung cancer tumorigenicity to a greater extent than the lower dosage (Supplemental Figure 2).

Bioinformatic mRNA targets. To study mechanisms responsible for lung cancer growth suppression caused by miR-31 knockdown, we performed bioinformatic analyses to search for miR-31 target mRNAs. TargetScan 4.1, PicTar, and miRanda were each used to independently predict miR-31 targets. It is known that each miRNA can affect multiple targets via distinct mechanisms (29). Given this, attention focused on identification of candidate tumor-suppressive genes that could exert miR-31 growth-inhibitory effects. Several candidates were highlighted, including LATS2, PPP2R2A, Frizzled homolog 3 (FZD3), Sprouty-related, EVH1 domain containing 1 (SPRED1), Sprouty homolog 4 (SPRY4), AXIN1 upregulated 1 (AXUD1), and DICER1. These candidate targets were validated based on (a) an inverse relationship between miR-31 and their expression in murine as well as human lung cancers; (b) experiments revealing that in vitro growth inhibition by engineered miR-31 repression was antago-

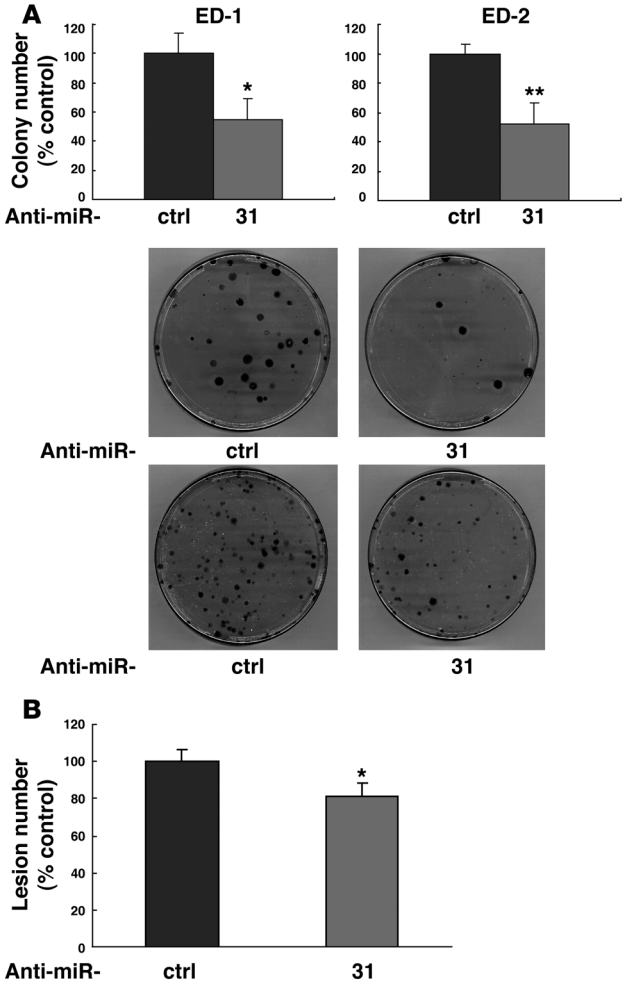

Figure 5

Repression of miR-31 expression significantly affects murine lung cancer clonal growth and tumorigenicity. (**A**) Colony formation was suppressed in ED-1 and ED-2 murine lung cancer cells relative to controls by engineered knockdown of miR-31 through transient anti–miR-31 transfection. The stained colonies are displayed in the bottom row. (**B**) Repression of in vivo lung tumorigenicity of the indicated transfected ED-1 cells after FVB mouse tail vein injections. The bars represent the percentage of lung lesion numbers for anti–miR-31 transfection of ED-1 cells relative to mice injected via tail vein with anti–miR-ctrl transfected ED-1 cells. Forty mice in total were used, and each group had 10 mice, with results pooled from 2 independent experiments, as described in Methods. $^{*}P \leq 0.05$, $^{**}P < 0.01$. Error bars indicate SD in **A** and SEM in **B**.

nized by knockdown of a putative target; and (c) evidence for direct binding in 3′-UTR luciferase reporter assays. The miR-31 targets sought were those that were repressed by forced miR-31 overexpression and augmented by its engineered knockdown in lung cancer cells. Among these candidates, only LATS2 and PPP2R2A satisfied this criterion (Figure 6, A and B) and the others. All 6 cell lines (ED-1, ED-2, C10, H23, H226, and BEAS-2B) were independently examined in these analyses, and studies yielded concordant results.

LATS2, human large tumor suppressor 2 (also known as KPM), is a member of the LATS tumor suppressor family (30). LATS2 was identified as exerting tumor-suppressive effects by inhibition of the G_1/S cell cycle transition (31). LATS2 was also found to be a target of miR-372 and miR-373 in testicular germ cell cancers (32). PPP2R2A, also known as protein phosphatase 2A B55 subunit, was previously uncovered as a tumor suppressor that induced apoptosis (33, 34).

LATS2 and PPP2R2A are direct miR-31 targets. Luciferase binding assays were conducted using pEZX-MT01 luciferase constructs to determine whether miR-31 suppressed LATS2 and PPP2R2A through direct binding to their respective 3′-UTRs. Wild-type and mutant 3′-UTRs of LATS2 or PPP2R2A were independently cloned into this vector containing the firefly luciferase gene, with the control *Renilla* luciferase gene driven by the CMV promoter. The ratios of firefly and *Renilla* luciferase signals reflected the degree of 3′-UTR binding of these targets.

The luciferase signals for wild-type 3′-UTR sequences of both LATS2 and PPP2R2A were repressed by cotransfection of pre–miR-31 in ED-1 cells and increased by cotransfection of anti–miR-31. In contrast, engineered mutations of the miR-31–binding site antagonized these effects (Figure 6, C and D). These results indicated that miR-31 can directly bind to the 3′-UTR sequences of LATS2 and PPP2R2A.

To determine whether LATS2 and PPP2R2A were engaged in miR-31–mediated growth suppression, we individually knocked down these target genes by siRNAs in ED-1 cells 48 hours after initial anti–miR-31 transfection to learn whether this would repress miR-31 effects. As expected, siRNA-mediated knockdown of either LATS2 or PPP2R2A antagonized growth suppression caused by engineered miR-31 repression (Figure 7A). Two different siRNAs were used to target LATS2 as well as to target PPP2R2A. Each study was conducted in triplicate, and the results were replicated in 2 independent experiments. Compared with control siRNAs, LATS2-targeting siRNAs and PPP2R2A-targeting siRNAs each repressed these respective mRNAs to levels 5%–6% of the basal expression levels as measured by real-time RT-PCR assays (Figure 7B). These results revealed that repression of LATS2 and PPP2R2A antagonized growth suppression caused by miR-31 knockdown and functionally validated them as miR-31 growth-regulatory targets. Similar results were independently obtained in experiments with ED-2 cells, as shown in Figure 7, C and D. Similar assays were conducted using the human lung cancer cell lines H226 and H23. As shown in Supplemental Figure 3, these results were concordant with findings obtained in murine lung cancer cells.

LATS2 and PPP2R2A expression in lung cancers. Since miR-31 was overexpressed in both murine cyclin E–driven transgenic lung cancers and human lung cancer tissues, we next examined whether LATS2 and PPP2R2A were each repressed in these lung cancers relative to adjacent normal lung tissues. Real-time RT-PCR assays were conducted on murine cyclin E–driven transgenic lung adenocarcinomas and adjacent normal lung tissues, as well as in previously examined paired human normal-malignant lung tissues (17). LATS2 and PPP2R2A were each basally repressed in these murine transgenic lung cancers, with mRNA levels significantly reduced as compared with those in adjacent normal lung tissues, as shown in Figure 8, A and B. As expected, LATS2 and PPP2R2A expression profiles were also repressed in all examined human lung cancers relative to adjacent normal tissues, as shown

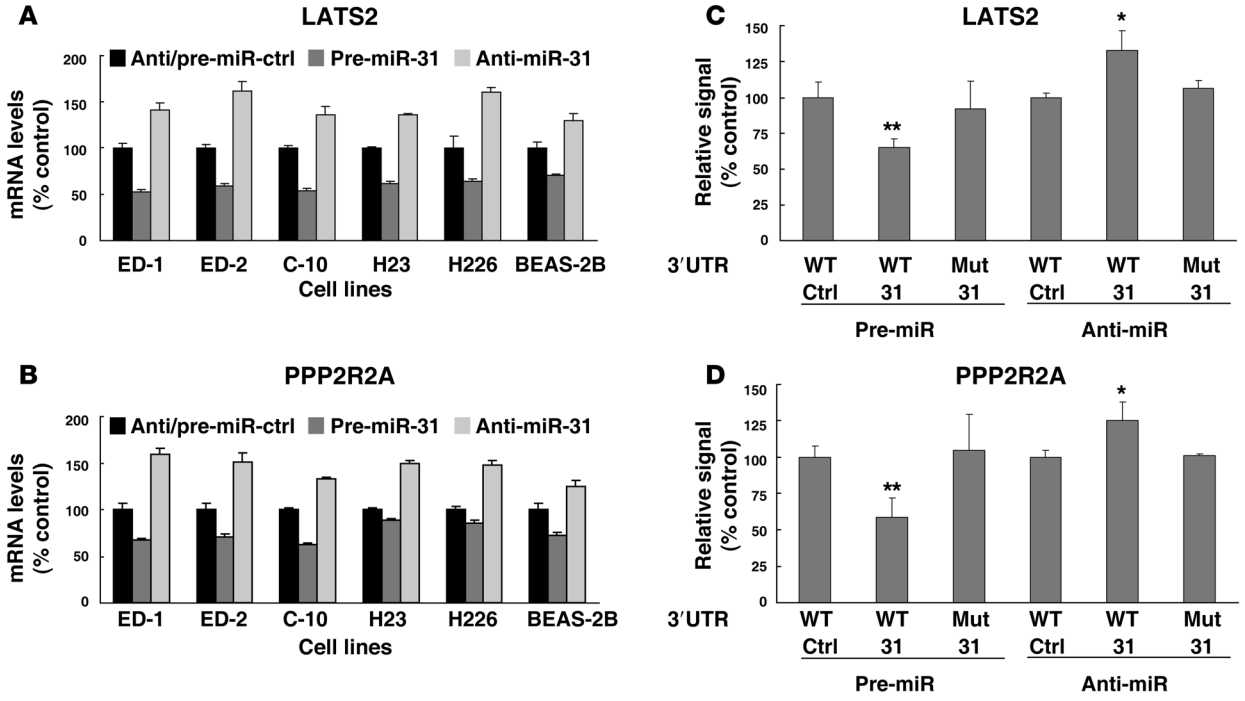

Figure 6

LATS2 and PPP2R2A are miR-31 target mRNAs. Real-time RT-PCR assays confirmed that (**A**) LATS2 and (**B**) PPP2R2A expression levels were each downregulated by pre–miR-31 and upregulated by anti–miR-31 transfections independently performed in ED-1, ED-2, C-10, H23, H226, and BEAS-2B cells. All transfectant groups in **A** and **B** had *P* values less than 0.0001. The described 3′-UTR luciferase binding assays confirmed that miR-31 binds to the wild-type 3′-UTR sequences of (**C**) LATS2 and (**D**) PPP2R2A in ED-1 cells. Cotransfection of pre–miR-31 significantly reduced the luciferase levels, and cotransfection of anti–miR-31 increased them. In contrast, a mutated miR-31–binding site (Mut) within these 3′-UTRs antagonized these effects. $*P < 0.05$, $**P < 0.01$. Error bars indicate SD.

in Figure 8, C and D. These results establish that expression profiles were concordant for miR-31 and its target mRNAs in both murine and human lung cancers.

Clinical associations between miR-31 and target genes. To comprehensively examine the clinical association between miR-31 and its target genes (LATS2 and PPP2R2A), we examined a human lung cancer tissue microarray and mRNA isolated from corresponding cases using samples from patients identified through the New Hampshire State Cancer Registry and the Dartmouth-Hitchcock Tumor Registry, as described in Methods. We conducted assays on this tissue microarray to examine cyclin E immunohistochemical expression and ISH analyses for miR-31. We also performed real-time RT-PCR assays on mRNA isolated from these tissues to determine levels of LATS2 and PPP2R2A. Cyclin E and miR-31 expression levels were significantly associated with each other ($P < 0.001$). According to a previously optimized scoring system (35), low miR-31 expression was associated with low levels of cyclin E, and intermediate and high miR-31 levels were associated with higher cyclin E levels (Figure 9A). Logistic regression analyses were used to explore the association between miR-31 expression profiles in malignant as well as normal lung tissues. Enhanced miR-31 expression was more frequent in malignant as compared with normal lung tissues, as shown in Figure 9B. This difference was particularly apparent in subjects with squamous cell carcinoma ($P = 0.048$). Real-time RT-PCR assays performed on mRNA harvested from the same cases also confirmed that levels of LATS2 and PPP2R2A were repressed in lung cancers as compared with normal lung tissues (Figure 9C). These results uncovered a close relationship between cyclin E and miR-31 expression as well as between miR-31 and expression of its target genes *LATS2* and *PPP2R2A* in human lung cancers.

Discussion

It is known that miRNAs are key regulators of gene expression and that these are aberrantly expressed in diverse cancers, including lung cancer (5, 9, 10, 17). Murine cyclin E–driven transgenic lines were studied as tools that recapitulated key features of human lung carcinogenesis (18). A set of miRNAs (miR-136, miR-376a, and miR-31) was prominently overexpressed in murine lung cancers versus adjacent normal lung tissues according to microarray and real-time RT-PCR assays. These miR-31 expression profiles were confirmed in murine and human lung tissues by real-time PCR and ISH assays (Figures 1 and 2 and Figure 3). Expression profiles for these highlighted miRNAs in murine malignant versus normal lung tissues were similar to those in a paired human normal-malignant lung tissue bank (Figure 3B). Engineered knockdown of miR-31 repressed proliferation of both murine and human lung cancer cell lines, but modest or no significant growth inhibition was observed in immortalized pulmonary epithelial cell lines, indicating differential inhibitory effects in these distinct cell contexts (Figure 4). Engineered repression of miR-31 also reduced lung cancer cell clonal growth and in vivo tumorigenicity in the lung (Figure 5). Notably, this repression of in vivo tumorigenicity depended on dose-dependent reduction of miR-31 expression (Supplemental Figure 2).

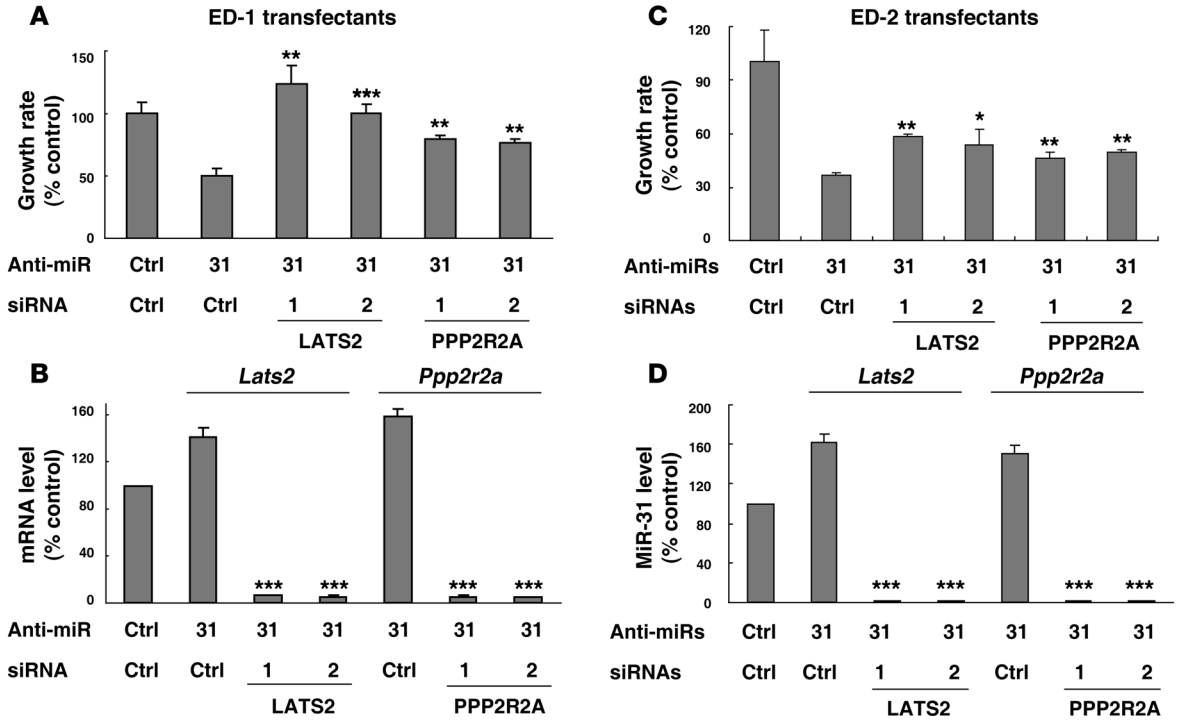

Figure 7
The proliferation of murine lung cancer cells following regulated expression of miR-31, LATS2, or PPP2R2A. The growth of (**A**) ED-1 cells and (**C**) ED-2 cells was suppressed by transfection of anti–miR-31. This was antagonized by either LATS2- or PPP2R2A-targeting siRNA transfections performed 48 hours after anti–miR-31 transfection. Two independent siRNAs were each used to target LATS2 as well as PPP2R2A. $^{*}P < 0.05$, $^{**}P < 0.01$, $^{***}P < 0.0001$. The mRNA levels of *Lats2* and *Ppp2r2a* are presented for the indicated transfectants in (**B**) ED-1 cells and (**D**) ED-2 cells following real-time RT-PCR assays. All results were normalized to the anti–miR-ctrl and the negative control siRNA transfectants. $^{***}P < 0.0001$. Error bars indicate SD.

In studying potential mechanisms engaged, we identified LATS2 and PPP2R2A as tumor-suppressive mRNA targets by bioinformatic analyses and functional as well as binding assays. Both target mRNAs were downregulated by miR-31 (Figure 6). Knockdown of miR-31 augmented LATS2 and PPP2R2A expression and conferred growth inhibition, which was antagonized by siRNA-mediated knockdown of either LATS2 or PPP2R2A (Figure 7). Expression levels of LATS2 and PPP2R2A were each basally repressed in both murine and human lung cancer cells (Figure 8). Clinical associations between miR-31 and its target genes, *LATS2* and *PPP2R2A*, were uncovered (Figure 9 and data not shown). Taken together, these findings revealed a set of miRNAs prominently overexpressed in lung cancers, and of these species, only miR-31 was functionally required to drive lung cancer cell growth and tumorigenicity. These findings build on previously highlighted growth-suppressive miRNAs in lung cancer (17) by revealing specific miRNAs overexpressed in lung cancer. We propose that miR-31 acts as an oncomir in this context by negatively regulating specific tumor suppressors. This view is supported by miR-31 knockdown experiments in which its tumor-suppressive targets, LATS2 and PPP2R2A, were derepressed. Thus, the miR-31/LATS2/PPP2R2A pathway constitutes a previously unrecognized growth regulator of lung cancer.

Lung cancer is the leading cause of cancer mortality for men and women in the United States (8). An improved understanding of lung cancer biology and therapy is needed. This study advances prior work (6, 7, 9–17) by uncovering the key role played by miR-31 in regulating lung carcinogenesis and by finding functionally relevant mRNA targets. Future work should build on these findings by precisely determining how these tumor-suppressive pathways are activated by miR-31 repression and how augmented LATS2 and PPP2R2A expression confers repression of lung cancer growth in vitro and in vivo. Preliminary studies indicated that changes in cell cycle regulation may confer some of the observed anti-neoplastic effects (data not shown).

The miRNAs are promising anti-neoplastic agents (36). It is appealing to consider testing an inhibitor to a functionally important oncogenic miRNA (such as miR-31) for treatment of transgenic lung cancer models or other murine cancer models to learn whether this would elicit antitumor responses. In this regard, the wild-type and proteasome degradation–resistant cyclin E–transgenic lines studied here should prove useful for prioritizing miRNAs for further study as clinical anti-neoplastic agents. Perhaps combination therapy with pharmacologically optimized inhibitors of miR-31 will confer desired antitumorigenic effects. The miR-17-92 and miR-200/429 families are also important in lung cancer biology (37, 38), and their inhibitors might cause anti-neoplastic effects. This might involve both knockdown of an oncomir and overexpression of a tumor-suppressive miRNA in lung cancer. Successful preclinical studies would set the stage for clinical targeting of highlighted miRNAs. Notably, in vitro and in vivo reports of LNA-mediated silencing of miRNAs support the use of LNAs for targeting specific miRNAs (39, 40).

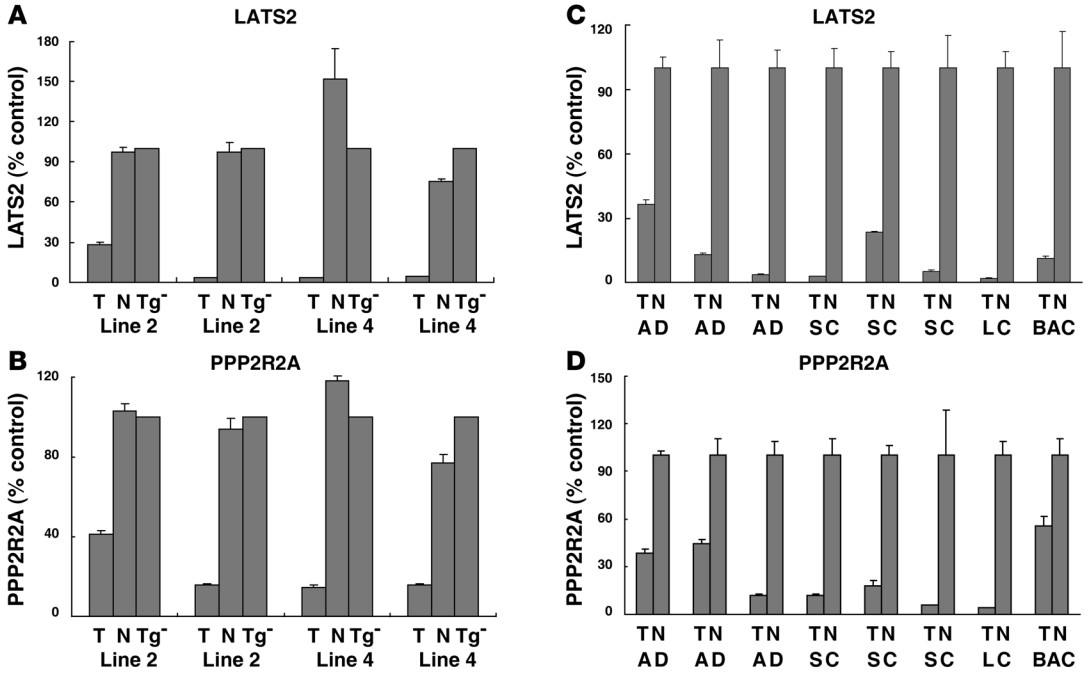

Figure 8

Validation of LATS2 and PPP2R2A expression profiles by real-time RT-PCR assays performed on RNA isolated from the indicated murine cyclin E–transgenic lines and from the paired human normal-malignant lung tissues. Real-time RT-PCR assays for (**A**) LATS2 and (**B**) PPP2R2A were performed. Results were normalized to expression within nontransgenic FVB mouse lung tissues. Real-time RT-PCR assays for (**C**) LATS2 and (**D**) PPP2R2A were independently performed on paired human normal-malignant lung tissues. Results were normalized to expression in normal human lung tissues. In all groups, *P* values were less than 0.001. Error bars indicate SD.

In summary, miR-136, miR-376a, and miR-31 were prominently overexpressed miRNAs in murine and human lung cancers relative to adjacent normal lung tissues. Engineered repression of miR-31, but not the other 2 miRNAs, caused marked repression of lung cancer growth in vitro and in vivo. Notably, LATS2 and PPP2R2A were targeted by miR-31, providing a likely mechanism responsible for the observed growth inhibition through a previously unrecognized regulation of tumor-suppressive pathways. It is intriguing to speculate that use of miR-31 as a biomarker would improve diagnosis or classification of human lung cancer and even provide prognostic information. In this regard, preliminary data indicated a trend toward poor prognosis in lung cancer cases exhibiting high miR-31 expression (data not shown). Conceivably, targeting of miR-31 by anti-miR oligonucleotides would form the basis for a novel strategy to treat or even prevent different types of lung cancers. Indeed, evidence indicated that clinical associations exist between miR-31 and cyclin E in NSCLC subtypes beyond adenocarcinoma, where these associations were first found. Taken together, these findings indicate that miR-31 acts as an oncogenic miRNA in lung cancer by conferring repression of specific tumor suppressors.

Methods

Transgenic lung tissues. Murine cyclin E–transgenic lines that exhibit premalignant and malignant (adenocarcinoma) lung lesions were previously described (18). Those studied here included human SP-C–driven wild-type cyclin E–transgenic (line 2) and proteasome degradation–resistant (line 4) lines (18). Adenocarcinomas and adjacent histopathologically normal lung tissues were individually harvested from age- and sex-matched mice and immediately placed in RNAlater (Ambion). Total RNA was isolated using established techniques (17, 35, 41) for miRNA expression arrays. Formalin-fixed and paraffin-embedded transgenic lung tissues were harvested (18) and used for ISH assays.

Human lung tissues. Paired human normal and malignant lung tissues were obtained after review and approval by Dartmouth's Institutional Review Board (IRB). Patient identifying information was not linked to this tissue bank consecutively accrued over 8 years at Dartmouth-Hitchcock Medical Center (17).

RNA isolation and miRNA arrays. The RNA isolation and miRNA array procedures were described previously (17). In brief, total RNA was isolated from cell lines and lung tissues with TRIzol reagent (Invitrogen) and was 3′-end labeled using T4 RNA ligase to couple Cy3-labeled RNA linkers. Labeled RNA was hybridized to LNA microarrays overnight at 65°C in a hybridization mixture containing 4× sodium chloride sodium citrate (SSC) (1× SSC: 150 mM sodium chloride and 15 mM sodium citrate), 0.1% SDS, 1 μg/μl herring sperm DNA, and 38% formamide. Slides were washed 3 times in 2× SSC, 0.025% SDS at 65°C, 3 times in 0.8× SSC, and 3 times in 0.4× SSC at room temperature. Each RNA sample was independently hybridized twice. There were 4 probe sets used for each miRNA. Only concordant hybridization results were scored. Microarrays were scanned using an ArrayWorx scanner (Applied Precision). Images were analyzed using GridGrinder (http://gridgrinder.sourceforge.net/), and background-subtracted spot intensities were normalized using variance stabilization normalization (35). The miRNAs selected for in-depth study showed statistically significant expression differences in both murine and human normal versus malignant lung tissues.

Real-time RT-PCR assays. The miRNA RT-PCR assays were performed using the TaqMan miRNA Reverse Transcription Kit (Applied Biosys-

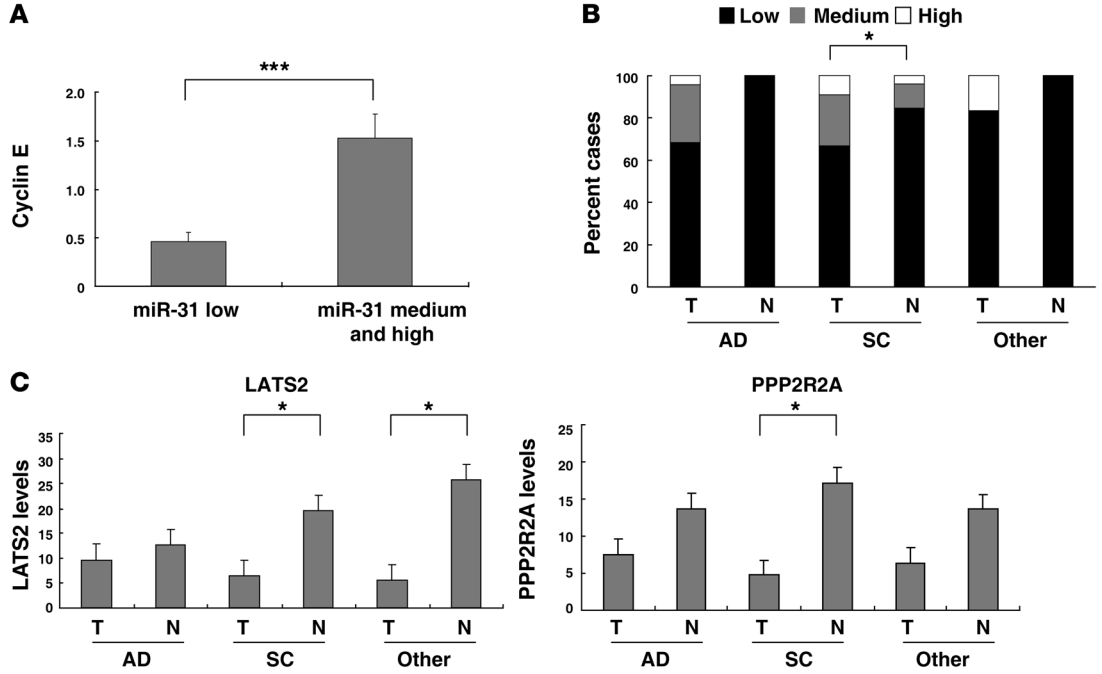

Figure 9
Clinical associations between miR-31 expression profiles and those of its target genes, *LATS2* and *PPP2R2A*, were explored as described in Methods. (**A**) Associations between cyclin E immunohistochemical expression and miR-31 levels were significant. (**B**) Augmented miR-31 expression was more frequent in malignant as compared with normal lung tissues. (**C**) LATS2 and PPP2R2A were significantly downregulated in lung cancers as compared with adjacent normal lung tissues. "Other" indicates lung cancer histopathologies. Error bars indicate SEM in **A** and SD in **B** and **C**. $^{*}P < 0.05$, $^{***}P < 0.0001$.

tems) and the 7500 Fast Real-Time PCR System (Applied Biosystems) for quantitative miRNA detection, and each miRNA TaqMan PCR probe was purchased from Applied Biosystems, as described previously (17). The real-time RT-PCR assays were performed using the 7500 Fast Real-Time PCR System for quantitative mRNA detection and with iTaq Fast SYBR Green Supermix (Bio-Rad). The primers for real-time PCR were human GAPDH: 5′-ATGGGGAAGGTGAAGGTCG-3′ (forward) and 5′-GGGGTCATTGATGGCAACAATA-3′ (reverse); human PPP2R2A: 5′-TCGGATGTAAAATTCAGCCA-3′ (forward) and 5′-CATGCACCTGGTATGTTTCC-3′ (reverse); human LATS2: 5′-CAGATTCAGACCTCTCCCGT-3′ (forward) and 5′-CTTAAAGGCG-TATGGCGAGT-3′ (reverse); mouse GAPDH: 5′-AGGTCGGTGTGAAC-GGATTTG-3′ (forward) and 5′-TGTAGACCATGTAGTTGAGGTCA-3′ (reverse); mouse LATS2: 5′-AGCAGATTGTGCGAGTCATC-3′ (forward) and 5′-GTGGTAGGATGGGAGTGCTT-3′ (reverse); mouse PPP2R2A: 5′-TAAGAGAGCGGTCCATTGTG-3′ (forward) and 5′-ACAGCTTTCTC-CATGAGGCT-3′ (reverse).

ISH assays. ISH assays were performed as in previous work (17, 35). In brief, slides were prehybridized in hybridization solution (50% formamide, 5% SSC, 500 μg/ml yeast tRNA, and 1% Denhardt's solution) at 50°C for 30 minutes. Ten picomoles of the desired FITC-labeled, LNA-modified DNA probes (Integrated DNA Technologies) complementary to specific miRNAs and/or biotinylated unmodified DNA probes against 18S rRNA were added and hybridized for 2 hours at a temperature 20–25°C below the calculated melting temperature of the LNA probe. After stringent washes, a tyramide signal amplification (TSA) reaction was carried out using the GenPoint Fluorescein kit (DakoCytomation) and the manufacturer's recommended procedures and with the substitution of streptavidin/HRP (Invitrogen) for detection of biotinylated probes. Slides were mounted with Prolong Gold solution (Invitrogen). This methodology was applied to the tissue array developed from the New Hampshire State Cancer Registry and the Dartmouth-Hitchcock Tumor Registry. The miR-31 levels were scored as low, medium, or high using a previously described ISH scoring system (35).

Cell lines. The murine lung cancer cell lines (ED-1 and ED-2) were derived from wild-type cyclin E– and proteasome degradation–resistant cyclin E–transgenic mice, respectively (17). The C10 murine alveolar type II epithelial cell line and H226, H23, HOP62, H522, and A549 human lung cancer cell lines were each purchased from ATCC. BEAS-2B immortalized human bronchial epithelial cells were provided by Curtis C. Harris (NIH and National Cancer Institute, Bethesda, Maryland).

Tissue culture. ED-1, ED-2, H226, H23, HOP62, H522, and A549 cells were each cultured in RPMI 1640 medium with 10% FBS and 1% antibiotic and antimycotic solution in a humidified incubator at 37°C in 5% CO_2. C10 cells were cultured in CMRL 1066 medium (Life Technologies) with 10% FBS, 2 mM L-glutamine, 100 U/ml penicillin, and 100 μg/ml streptomycin (18). BEAS-2B cells were cultured in serum-free LHC-9 medium (Invitrogen), as reported (42).

Transient transfection. ED-1, ED-2, C10, H226, H23, and BEAS-2B cells were individually plated subconfluently onto each well of 6-well tissue culture plates or 10-cm dishes 24 hours before transfection. Transient transfection of pre-miR miRNA precursors and/or anti-miR and control oligonucleotides (anti–miR-ctrl or pre–miR-ctrl) (Ambion) at a final concentration of 50 nM (or 200 nM) was accomplished with siPORT NeoFX reagent (Ambion) using previously optimized methods (17). The siRNA transfections were conducted following the same procedure as for a pre-miR and used at a final concentration of 25 nM. The Silencer Select Predesigned siRNAs were purchased from Applied Biosystems, and murine

LATS2 siRNAs (catalog 4390771 with siRNA ID s78350 and s78351), murine PPP2R2A siRNAs (catalog 4390771 with siRNA ID s90396 and s90395), human LATS2 siRNA (catalog 4392420 with siRNA ID s25503 and s25504), human PPP2R2A siRNA (catalog 4390824 with siRNA ID s608 and s609), and a negative control siRNA (catalog 4390843) were also used in these experiments. Logarithmically growing transfectants were harvested for independent immunoblot, proliferation, apoptosis, and trypan blue viability assays, as described below.

Proliferation and colony formation assays. The CellTiter-Glo proliferation assay (Promega) was used along with previously optimized methods (17). The colony formation assay was performed as in previous work (42) with 2.5×10^2 ED-1 cells or 5×10^2 ED-2 cells or the indicated transfectants independently plated onto 10-cm tissue culture plates. After 10 days, visible colonies were fixed and stained with Diff-Quik solution (Baxtor) and quantified using the Col Count instrument (Oxford Optronix), as previously described (17).

Apoptosis assay. Trypan blue viability assays were performed as described previously (28). Apoptosis was scored by annexin V:FITC positivity as detected by flow cytometry using the Annexin V assay kit (AbD Serotec) and following the vendor's recommended protocol.

In vivo tumorigenicity and statistical assays. Early passages of ED-1 cells were harvested in PBS supplemented with 10% mouse serum (Invitrogen), and 10^6 cells of each transfectant of this cell line were individually injected into tail veins of each respective FVB syngeneic mouse. In each experimental arm, 10 mice tail vein–injected with control transfected ED-1 cells and 10 mice tail vein–injected with miR-31–knockdown ED-1 transfectants were used (the final concentrations of anti–miR-31 and anti–miR-ctrl were each 50 nM). With a replicate experiment, a total of 40 mice were examined. After injection (17 days), mice were sacrificed according to an IACUC-approved protocol at Dartmouth, and harvested lung tissues were formalin fixed, paraffin embedded, sectioned, and H&E stained for histopathologic analyses using optimized methods (18). Histopathologic sections were scored for lung tumors by a pathologist who was unaware of the treatment arms being analyzed. The log transformation of these data was used to eliminate the skewness of counts, with the subsequent application of the 2-tailed *t* test for comparison of the number of lung lesions in the FVB mice injected with anti–miR-ctrl versus anti–miR-31 transfectants. The difference was scored as statistically significant if the *P* value was 0.05 or less. For an independent statistical analysis, the likelihood ratio test was used, with the assumption that counts follow a Poisson distribution. Computations were conducted using the statistical package S-Plus 6.1 (Insightful Inc.).

The dose-dependent in vivo tumorigenicity assays (Supplemental Figure 2) were conducted using the same experimental procedures as described above. For each experimental arm, up to 6 FVB mice were used. In these respective experiments, 50 nM (1-fold) and 200 nM (4-fold) final dosages of anti–miR-31 or anti–miR-ctrl were used. The same tumorigenicity scoring methods and statistics were used in each experiment.

Immunohistochemistry assays. The immunohistochemistry assays were conducted on tissue microarrays (described below) to detect and score cyclin E immunohistochemical expression profiles using previously optimized methods (18).

Bioinformatics. The following online software programs were used: TargetScan 4.1 (http://targetscan.org/vert_40/), Pictar (http://pictar.mdc-berlin.de/), and miRanda (http://cbio.mskcc.org/cgi-bin/mirnaviewer/mirnaviewer.pl).

3′-UTR luciferase binding assays. Murine LATS2 (MmiT031281-MT01), PPP2R2A (MmiT035372-MT01), and control (CmiT000001-MT01) 3′-UTR luciferase constructs were purchased from GeneCopoeia. The underlined sequences indicate the miR-31–binding site for LATS2 (TCTTGCC) and PPP2R2A (TGCACCATCTTGCC). These were mutated using the QuickChange XL Site-Directed Mutagenesis Kit (Stratagene). The resulting mutant binding sites for LATS2 (TCT**GCGG**) and for PPP2R2A (TGCACCATCT**GCGG**) are each indicated in bold.

Transient transfection of luciferase plasmids with pre-miR miRNA precursors and/or with an anti-miR inhibitor was conducted using Lipofectamine 2000 (Invitrogen) at final concentrations of 250 pg/μl (luciferase plasmid) and 50 nM (pre-miR or anti-miR). The luciferase signal was read by a TD-20/20 Luminometer (Turner Biosystems).

New Hampshire State Cancer and Dartmouth-Hitchcock Tumor Registries. The New Hampshire State Cancer Registry and the Dartmouth-Hitchcock Tumor Registry were used to identify persons from 2005 to 2007 who had received a clinical diagnosis of lung cancer. Eligible cases had histologically confirmed primary incident lung cancer, were between 30 and 74 years of age, resided in one of the 10 study counties, were alive at first contact, had a working telephone number, and were able to communicate in English. Of the eligible cases, 5% could not be reached because of an inaccurate address or phone number, 11% were too ill to be interviewed, and 22% refused to participate, which yielded a 61% participation rate. Survival status was determined using a combination of the National Death Index (deaths through 2006) and the Social Security Death Index (deaths through September 17, 2009). Tumor stage and histology were obtained from the State Cancer Registry. The signed consents were obtained to allow access to tumor specimens from these cases, and these studies were reviewed and approved by the Dartmouth IRB for human subjects. A master tissue microarray block was constructed containing tissue samples representing 84 subjects who had lung biopsies. The stage distribution of these cases was 50% stage I, 17% stage II, 20% stage III, 7% stage IV, and 5% unknown. The histopathology indicated 52% adenocarcinomas, 28% squamous cell cancers, 7% large cell cancers, 4% neuroendocrine cancers, and 9% unknown. The cases had a median age of 62, and 94% were current or former smokers with a median of 45 pack-years of smoking. These characteristics were similar to those of the overall study case group.

Note added in proof. After submission of our manuscript, a role for miR-31 in regulating breast cancer metastasis was reported (43).

Acknowledgments

This work was supported by NIH and National Cancer Institute (NCI) grants R01-CA087546 (to E. Dmitrovsky), R01-CA111422 (to E. Dmitrovsky), and R03-CA130102 (to E. Dmitrovsky); a Samuel Waxman Cancer Research Foundation Award (to E. Dmitrovsky); a grant from the American Lung Association (to X. Liu); an American Cancer Society Institutional grant (to S.J. Freemantle); a Danish National Advanced Technology Foundation Grant and a Danish Medical Research Council Grant (to S. Kauppinen); a postdoctoral fellowship (PDF0503563) grant from the Susan G. Komen Breast Cancer Foundation (to L.F. Sempere); and a Hitchcock Foundation grant (to L.F. Sempere). The Wilhelm Johannsen Center for Functional Genome Research is established by the Danish National Research Foundation. Ethan Dmitrovsky is an American Cancer Society Clinical Research Professor supported by a generous gift from the F. M. Kirby Foundation.

Received for publication April 16, 2009, and accepted in revised form January 13, 2010.

Address correspondence to: Ethan Dmitrovsky, Department of Pharmacology and Toxicology, Dartmouth Medical School, Hanover, NH 03755. Phone: 603.650.1707; Fax: 603.650.1129; E-mail: ethan.dmitrovsky@dartmouth.edu.

1. Calin GA, Croce CM. MicroRNA signatures in human cancers. *Nat Rev Cancer*. 2006;6(11):857–866.
2. Garzon R, Fabbri M, Cimmino A, Calin GA, Croce CM. MicroRNA expression and function in cancer. *Trends Mol Med*. 2006;12(12):580–587.
3. Zeng Y. Principles of micro-RNA production and maturation. *Oncogene*. 2006;25(46):6156–6162.
4. Valencia-Sanchez MA, Liu J, Hannon GJ, Parker R. Control of translation and mRNA degradation by miRNAs and siRNAs. *Genes Dev*. 2006; 20(5):515–524.
5. Esquela-Kerscher A, Slack FJ. Oncomirs — microRNAs with a role in cancer. *Nat Rev Cancer*. 2006;6(4):259–269.
6. Jay C, Nemunaitis J, Chen P, Fulgham P, Tong AW. miRNA profiling for diagnosis and prognosis of human cancer. *DNA Cell Biol*. 2007;26(5):293–300.
7. Hu Z, et al. Genetic variants of miRNA sequences and non-small cell lung cancer survival. *J Clin Invest*. 2008;118(7):2600–2608.
8. Jemal A, et al. Annual report to the nation on the status of cancer, 1975-2005, featuring trends in lung cancer, tobacco use, and tobacco control. *J Natl Cancer Inst*. 2008;100(23):1672–1694.
9. Takamizawa J, et al. Reduced expression of the let-7 microRNAs in human lung cancers in association with shortened postoperative survival. *Cancer Res*. 2004;64(11):3753–3756.
10. Yanaihara N, et al. Unique microRNA molecular profiles in lung cancer diagnosis and prognosis. *Cancer Cell*. 2006;9(3):189–198.
11. He L, et al. A microRNA polycistron as a potential human oncogene. *Nature*. 2005;435(7043):828–833.
12. Chang TC, et al. Widespread microRNA repression by Myc contributes to tumorigenesis. *Nat Genet*. 2008;40(1):43–50.
13. Corney DC, Flesken-Nikitin A, Godwin AK, Wang W, Nikitin AY. MicroRNA-34b and MicroRNA-34c are targets of p53 and cooperate in control of cell proliferation and adhesion-independent growth. *Cancer Res*. 2007;67(18):8433–8438.
14. Welch C, Chen Y, Stallings RL. MicroRNA-34a functions as a potential tumor suppressor by inducing apoptosis in neuroblastoma cells. *Oncogene*. 2007;26(34):5017–5022.
15. Tazawa H, Tsuchiya N, Izumiya M, Nakagama H. Tumor-suppressive miR-34a induces senescence-like growth arrest through modulation of the E2F pathway in human colon cancer cells. *Proc Natl Acad Sci U S A*. 2007;104(39):15472–15477.
16. Bommer GT, et al. p53-mediated activation of miRNA34 candidate tumor-suppressor genes. *Curr Biol*. 2007;17(15):1298–1307.
17. Liu X, et al. Uncovering growth-suppressive MicroRNAs in lung cancer. *Clin Cancer Res*. 2009;15(4):1177–1183.
18. Ma Y, et al. Transgenic cyclin E triggers dysplasia and multiple pulmonary adenocarcinomas. *Proc Natl Acad Sci U S A*. 2007;104(10):4089–4094.
19. Yu J, et al. Human microRNA clusters: genomic organization and expression profile in leukemia cell lines. *Biochem Biophys Res Commun*. 2006;349(1):59–68.
20. Veerla S, et al. MiRNA expression in urothelial carcinomas: important roles of miR-10a, miR-222, miR-125b, miR-7 and miR-452 for tumor stage and metastasis, and frequent homozygous losses of miR-31. *Int J Cancer*. 2009;124(9):2236–2242.
21. Slaby O, et al. Altered expression of miR-21, miR-31, miR-143 and miR-145 is related to clinicopathologic features of colorectal cancer. *Oncology*. 2007;72(5-6):397–402.
22. Gregory PA, Bracken CP, Bert AG, Goodall GJ. MicroRNAs as regulators of epithelial-mesenchymal transition. *Cell Cycle*. 2008;7(20):3112–3118.
23. Gregory PA, et al. The miR-200 family and miR-205 regulate epithelial to mesenchymal transition by targeting ZEB1 and SIP1. *Nat Cell Biol*. 2008;10(5):593–601.
24. Markou A, et al. Prognostic value of mature microRNA-21 and microRNA-205 overexpression in non-small cell lung cancer by quantitative real-time RT-PCR. *Clin Chem*. 2008;54(10):1696–1704.
25. Dixon-McIver A, et al. Distinctive patterns of microRNA expression associated with karyotype in acute myeloid leukaemia. *PLoS ONE*. 2008;3(5):e2141.
26. Lee JW, et al. Altered MicroRNA expression in cervical carcinomas. *Clin Cancer Res*. 2008;14(9):2535–2542.
27. Diederichs S, Haber DA. Sequence variations of microRNAs in human cancer: alterations in predicted secondary structure do not affect processing. *Cancer Res*. 2006;66(12):6097–6104.
28. Petty WJ, et al. A novel retinoic acid receptor beta isoform and retinoid resistance in lung carcinogenesis. *J Natl Cancer Inst*. 2005;97(22):1645–1651.
29. Bartel DP. MicroRNAs: target recognition and regulatory functions. *Cell*. 2009;136(2):215–233.
30. Kamikubo Y, Takaori-Kondo A, Uchiyama T, Hori T. Inhibition of cell growth by conditional expression of kpm, a human homologue of Drosophila warts/lats tumor suppressor. *J Biol Chem*. 2003;278(20):17609–17614.
31. Li Y, Pei J, Xia H, Ke H, Wang H, Tao W. Lats2, a putative tumor suppressor, inhibits G1/S transition. *Oncogene*. 2003;22(28):4398–4405.
32. Voorhoeve PM, et al. A genetic screen implicates miRNA-372 and miRNA-373 as oncogenes in testicular germ cell tumors. *Cell*. 2006;124(6):1169–1181.
33. Shtrichman R, Sharf R, Barr H, Dobner T, Kleinberger T. Induction of apoptosis by adenovirus E4orf4 protein is specific to transformed cells and requires an interaction with protein phosphatase 2A. *Proc Natl Acad Sci U S A*. 1999;96(18):10080–10085.
34. Roopchand DE, Lee JM, Shahinian S, Paquette D, Bussey H, Branton PE. Toxicity of human adenovirus E4orf4 protein in Saccharomyces cerevisiae results from interactions with the Cdc55 regulatory B subunit of PP2A. *Oncogene*. 2001;20(38):5279–5290.
35. Sempere LF, et al. Altered MicroRNA expression confined to specific epithelial cell subpopulations in breast cancer. *Cancer Res*. 2007;67(24):11612–11620.
36. Osaki M, Takeshita F, Ochiya T. MicroRNAs as biomarkers and therapeutic drugs in human cancer. *Biomarkers*. 2008;13(7):658–670.
37. Hayashita Y, et al. A polycistronic microRNA cluster, miR-17-92, is overexpressed in human lung cancers and enhances cell proliferation. *Cancer Res*. 2005;65(21):9628–9632.
38. Gregory PA, et al. The miR-200 family and miR-205 regulate epithelial to mesenchymal transition by targeting ZEB1 and SIP1. *Nat Cell Biol*. 2008;10(5):593–601.
39. Elmen J, et al. LNA-mediated microRNA silencing in non-human primates. *Nature*. 2008;452(7189):896–899.
40. Elmen J, et al. Antagonism of microRNA-122 in mice by systemically administered LNA-antimiR leads to up-regulation of a large set of predicted target mRNAs in the liver. *Nucleic Acids Res*. 2008;36(4):1153–1162.
41. Cole K, Truong V, Barone D, McGall G. Direct labeling of RNA with multiple biotins allows sensitive expression profiling of acute leukemia class predictor genes. *Nucleic Acids Res*. 2004;32(11):e86.
42. Feng Q, et al. UBE1L causes lung cancer growth suppression by targeting cyclin D1. *Mol Cancer Ther*. 2008;7(12):3780–3788.
43. Valastyan S, et al. A pleiotropically acting microRNA, miR-31, inhibits breast cancer metastasis. *Cell*. 2009;137(6):1032–1046.